Preoperative Computer Simulation and Patient-specific Guides are Safe and Effective to Correct Forearm Deformity in Children

Andrea S. Bauer, MD, Dora A. R. Storelli, MD,† Sarah E. Sibbel, MD,‡ H. Relton McCarroll, MD,† and Lisa L. Lattanza, MD†*

Background: Posttraumatic and congenital forearm deformities in children can be difficult to appreciate in all planes. In cases of distal radioulnar joint instability and loss of forearm rotation, surgical correction is challenging. Advances in 3-dimensional printing allow creation of custom guides at a reasonable cost, enabling precise correction of the deformity in all planes.

Methods: Nineteen children with deformity of the forearm had corrective osteotomies performed using preoperative 3-dimensional computer modeling and patient-specific surgical guides. Surgicase software was used for 3-dimensional planning of the corrective osteotomy, by superimposing a mirror image of the unaffected side as a template. Based upon this planning, patient-specific surgical guides were manufactured. Radiographic and clinical outcomes were assessed.

Results: Three patients had a diagnosis of multiple hereditary exostoses, and one of Madelung's deformity. The remaining 15 patients had a diagnosis of fracture malunion. Average preoperative angulation of both the radius and ulna was 23 degrees. For the patients with fracture malunions, the time from injury to surgery ranged from 6 months to 8 years. Twelve patients underwent osteotomies of both the radius and ulna, 5 had osteotomies of the radius alone, and 2 had a single osteotomy of the ulna only. All osteotomies went on to unite and no patient lost range of motion. Preoperative arc of forearm rotation averaged 101 degrees (range 0 to 180 degrees). Postoperatively, this improved to 133 degrees (range 85 to 180 degrees). Eight patients had distal radioulnar instability preoperatively, all of which normalized after surgery. There were 4 complications: 1 hypertrophic scar, 1 subject with extensor pollicis longus weakness, and 2 transient sensory losses in the superficial radial nerve distribution.

Conclusions: This case series demonstrates that 3-dimensional computer modeling permits complex and multiple osteotomies to be done safely to achieve deformity correction in children. Limitations in forearm rotation and distal radioulnar malalignment can be reliably improved using this technique.

Level of Evidence: Level IV—retrospective case series.

Key Words: computer-aided design, 3-dimensional model, forearm malunion, pediatric malunion, DRUJ instability

(*J Pediatr Orthop* 2015;00:000–000)

Deformity correction is the mainstay of pediatric orthopaedics. There are several causes of deformity of the radius and ulna in children. These include congenital diagnoses (Madelung deformity, longitudinal deficiencies, congenital radial head dislocation), neuromuscular conditions (arthrogryposis, brachial plexus birth palsy), tumors (osteochondromas, Trevor disease), and trauma. It is commonly accepted that residual malunion after remodeling with angular deformity of >20 degrees and rotational deformity of >30 degrees in the forearm will lead to a noticeable difference in the arc of forearm rotation.[1,2]

Analysis of forearm deformity is, however, challenging. Simple angulation and translation of the radius and ulna can be viewed on plain radiographs, but rotational deformity can only be estimated. Common techniques are to look for the bicipital tuberosity to be approximately 180 degrees from the radial styloid on an anteroposterior radiograph of the forearm, as well as for the cortices above and below the fracture site to be the same width.[3,4] These "rules of thumb," however, are likely to miss subtle rotational malalignments. Computed tomography (CT) scanning and 3-dimensional modeling have the potential to enable clearer visualization of rotational deformities. Miyake and colleagues reviewed the characteristics of 15 forearm fracture malunions using CT-based 3-dimensional modeling. They found a range of rotational deformities, from 115 degrees of pronation to 15 degrees of supination, and concluded that osteotomies for these malunions must correct the deformity in all 3 dimensions.[5]

Just as analysis of the deformity is challenging, correction of deformity in the pediatric forearm can also be difficult. Fortunately, the majority of pediatric forearm malunions will remodel sufficiently over time to obviate the need for surgical correction. Children under 8 years

From the *Boston Children's Hospital, Boston, MA; †Shriners Hospitals for Children-Northern California, Sacramento, CA; and ‡Children's Hospital Colorado, Aurora, CO.

The authors did not, however, receive any funding or other support for this article.

The authors declare no conflicts of interest.

Reprints: Andrea S. Bauer, MD, Boston Children's Hospital, 300 Longwood Avenue, Boston, MA 02115. E-mail: andrea.bauer@childrens.harvard.edu.

old can be expected to remodel up to 20 degrees of diaphyseal angulation, 100% translation, and 1 cm of shortening.[6] Although residual angulation of >10 degrees is described in up to 50% of pediatric forearm fractures, these deformities are often well tolerated. Perhaps for this reason, there are not many published techniques for correction of these deformities.[6,7] Techniques based on plain radiographs require substantial intraoperative decision making.[8,9] This decision making can be complex when the deformity involves multiple sites or is in a critical location such as the distal radioulnar joint (DRUJ).

There is increasing use of 3-dimensional computer modeling in orthopaedics. In the adult upper extremity, 3-dimensional modeling combined with 3-dimensional printing of patient-specific drill guides allows precise correction of complex intra-articular distal radius fractures.[10] A randomized clinical trial is currently underway to determine whether this careful preoperative planning indeed translates into improved postoperative outcomes for complex distal radius fractures.[11] Kataoka et al[12] have shown that a similar technique of 3-dimensional computer modeling and 3-dimensional printing of guides can reliably correct adult diaphyseal forearm fracture malunions.

The purpose of this study is to present our early experience using preoperative 3-dimensional modeling and patient-specific guides to correct deformities of the pediatric forearm and improve forearm rotation and/or DRUJ stability. Our results demonstrate that this technique is safe, effective, and allows for precise correction of complex deformities that would otherwise be more difficult to correct and with less predictable outcomes.

METHODS

Record Review

We retrospectively reviewed 19 consecutive children who underwent forearm osteotomies using patient-specific guides created with 3-dimesional printing between August 2012 and November 2014. Indications for surgery included forearm deformity with limitation in pronosupination, DRUJ instability, or both. All children were followed at least until union of the osteotomies. Medical records were searched for demographics and surgical data, as well as preoperative and postoperative range of motion (ROM) and DRUJ stability. All ROM measurements were performed using a goniometer. DRUJ stability was recorded as a yes/no variable only. No patients were excluded during this consecutive series, and no patient was lost to follow-up.

Radiographic Evaluation

Radiographic union was achieved when no osteotomy lines were visible on plain radiographs. The most recent radiograph immediately preceding surgery was designated the "preoperative" radiograph, and the first radiograph to demonstrate union across all osteotomy sites was designated the "postoperative" radiograph. Preoperative and postoperative radiographs were measured using PACS (Picture Archiving and Communication System) software (McKesson, San Francisco, CA) to determine angulation of the radius and ulna before and after surgery.

For posttraumatic cases, the shaft-to-shaft angulation at the fracture site was measured on anteroposterior radiographs to obtain the coronal angulation of both the radius and the ulna, and the same measurement was taken on the lateral radiographs to obtain the sagittal angulation of each bone. The largest of these 4 numbers was designated the "maximum angulation." For nontraumatic cases, these measurements were taken at the center of rotation of angulation of the deformity. We also noted whether there was an obvious rotational deformity of the radius or ulna, meaning that either the bicipital tuberosity was clearly not opposite the radial styloid, or the bone cortices above and below the fracture site were of clearly different widths. For comparison, the 3-dimensional reconstructions were analyzed to determine how much rotation of each bone was actually required to match to the contralateral normal side. This was done by drawing a line from the radial styloid to the sigmoid notch on the axial projection of the 3-dimensional model of the preoperative state, and comparing this to the same line on the planned outcome model.

Surgical Technique

A bilateral axial CT scan of the forearm is performed, and the raw imaging (DICOM) data is uploaded to the Web site of Materialise NV (Leuven, Belgium). A clinical engineer at Materialise then uses the DICOM data to create a 3-dimensional model and superimposes a mirror image of the child's normal side onto the side with the deformity. The surgeon and engineer work together through video conferencing to plan virtual osteotomies to correct the side with the deformity. Generally, the engineer will start first, by identifying the point of maximal deformity and designing an osteotomy to correct the deformity at that location. The surgeon will then review the plan and decide whether additional cuts are needed, or whether the location of the osteotomy needs to be changed. Once final osteotomy sites are decided upon, the surgeon's preferred hardware specifications are added to the model, including locking versus nonlocking screws, and any necessary plate bending. Once the plan is finalized, the engineer designs patient-specific bone models, cutting guides, and drill guides, which are then printed on a 3-dimensional printer and shipped to the hospital. The drill guides are designed with the rotational and angular correction built in, so that once the osteotomies are completed, the placement of screws determines the correction. For the cases in this series, all radius osteotomies were performed through extensile volar approaches to the radius, and all ulnar osteotomies were performed through the subcutaneous approach to the ulna. The drill guides were used first, followed by the osteotomy guides, and all osteotomies were fixed with prechosen and prebent (when needed) plate and screw constructs. Figure 1 demonstrates

the process for a typical case in this series. It must be noted that the use of this system for osteotomy planning in children before skeletal maturity is considered "off-label" by the Food and Drug Administration.

Statistical Methods

The Wilcoxon signed-rank sum test with a significance level of $P < 0.05$ was used to determine differences between preoperative and postoperative forearm

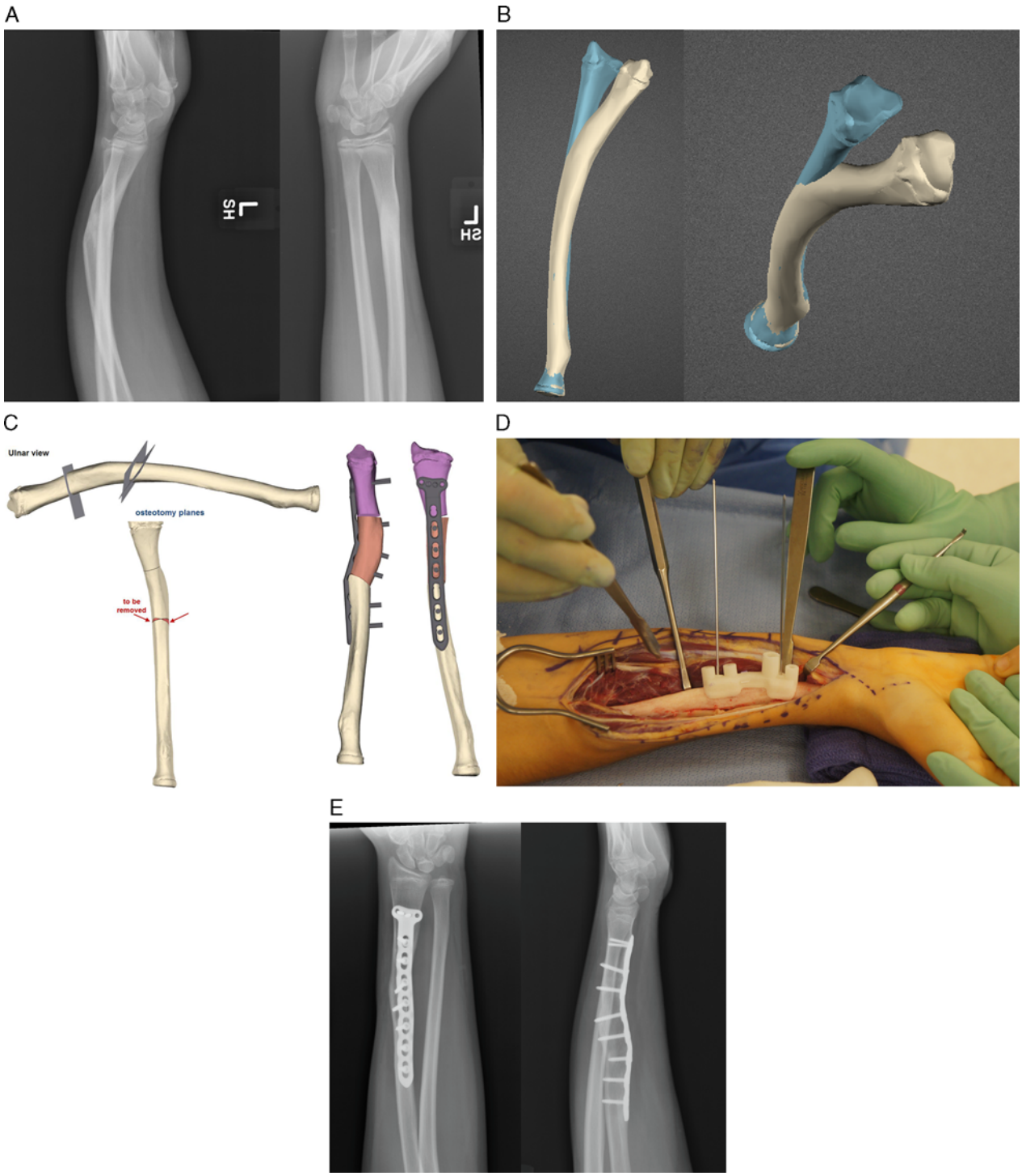

FIGURE 1. A, Preoperative radiograph demonstrating posttraumatic deformity. B, Three-dimensional computer model of the operative side (white) superimposed on a mirror image of the normal side (blue). C, Computer model of planned osteotomy and planned correction with hardware in place. D, Intraoperative photograph of the radius with a drill guide in place. E, Postoperative radiograph demonstrating correction.

rotation as well as differences between preoperative and postoperative radiographic measurements.

Institutional Review Board

This study was approved by our local Institutional Review Board.

RESULTS

Demographics

Our study group consisted of 19 subjects with a mean age of 13.5 years at the time of surgery. The etiology of the forearm deformity was posttraumatic in 15 cases, due to Madelung deformity in 1 case, and due to multiple hereditary exostoses (MHE) in 3 cases. Fourteen children had a limitation of forearm rotation preoperatively (total arc of forearm rotation <160 degrees), 8 children had instability of the DRUJ preoperatively, and 3 children had both problems. For the posttraumatic cases, the osteotomies were performed an average of 41 months after the initial fracture (Table 1).

Clinical Results

Two children had a single osteotomy of the radius only, 1 child had a single osteotomy of the ulna only, 4 children had double osteotomies of a single bone, and 12 children underwent osteotomies of both forearm bones (Table 2). One child had a radial head replacement placed at the same time as the osteotomy. The radial head replacement was performed to treat the radiocapitellar arthrosis that occurred due to malunion of the proximal radius. In that case, an osteotomy of the proximal radius was necessary to realign the radiocapitellar joint in order for replacement of the radial head to be possible. Another child had an external fixator placed for lengthening of the ulna at the same time as the guided osteotomy for treatment of a shortened ulna due to MHE. These 2 cases are included to show that this technique can be applied in a variety of situations. The mean arc of pronosupination for all subjects improved significantly after surgery from 101 to 137 degrees ($P = 0.017$) (Table 3). When only those 10 children who had limited pronosupination due to a fracture malunion were included, the mean arc of motion improved from 85 to 138 degrees. All 8 subjects with DRUJ instability had the instability resolve following surgery.

All cases went according to plan and we encountered no issues in using the guides. Four minor complications were noted. These included 2 transient superficial radial nerve palsies, 1 patient with transient weakness of the extensor pollicis longus, and 1 hypertrophic scar. In addition, 3 patients required longer than 6 months to reach complete bony union of the osteotomies. No major complications were noted. One child so far has elected to have the hardware removed and the 1 child with the external fixator has had the fixator removed.

TABLE 1. Demographics and Surgery Characteristics

	N (%)
Affected side	
Right	8 (42)
Left	11 (58)
Sex	
Male	12 (63)
Female	7 (37)
Age [mean (range)] (y)	13.5 (7.9-18.9)
Diagnosis	
Forearm malunion	15 (79)
Multiple hereditary exostoses	3 (16)
Madelung	1 (5)
Time from fracture to osteotomy [mean (range)] (mo)	41 (6-104)
Indication for surgery	
Limited forearm rotation	14 (74)
Distal radioulnar joint instability	8 (42)
Procedure	
Radius osteotomy only	5 (26)
Ulna osteotomy only	2 (11)
Both radius and ulna osteotomy	12 (63)
Status of physis	
Radial physis open at surgery	12 (63)
Ulnar physis open at surgery	10 (53)

Radiographic Results

On the preoperative radiographs, 12 children had open distal radial physes and 10 chlidren had open distal ulna physes. Seventeen of 19 subjects had an angular deformity of one or more forearm bones, with an average maximum angulation of 23 degrees (range 8 to 45 degrees). Three subjects had obvious rotational deformities on plain radiographs. For one of these, the widths of the cortices above and below the radius fracture were clearly different. In the other 2, the bicipital tuberosity was not opposite the radial styloid. Preoperative 3-dimensional modeling demonstrated that rotational correction of >10 degrees in the radius and/or the ulna was actually required in 17 cases (Fig. 2).

Postoperatively, no fixation devices crossed the physis. Radiographic union was seen at an average of 16 weeks after surgery (range 9 to 29 wk). The mean maximum angulation at the deformity improved significantly from 23 to 9 degrees in the radius and from 23 to 8 degrees in the ulna ($P = 0.003$ and 0.002, respectively) (Table 3). There were no hardware complications.

DISCUSSION

The advent of 3-dimensional printing has made routine use of computer modeling in orthopaedic surgery a reality. With our preoperative computer modeling, we revealed 14 rotational deformities that were not obvious on plain radiographs, allowing us to plan a more accurate correction than we otherwise would have done. This is similar to the recent study by Miyake and colleagues, in which the authors created 3-dimensional models of 21 forearm malunions, and found that a rotational component was present in 16 of them.

Before 3-dimensional printing, the translation of the computer model to the operating room was complex. Jupiter and colleagues reported on the use of CT image data and a computer-controlled milling machine to create bone models of complex distal radius malunions. The bone models were helpful for surgical planning, but did

TABLE 2. Individual Subject Characteristics

Subjects	Diagnosis	Age at Osteotomy (y)	Months After Fracture	Osteotomy Location	Preoperative Angular Deformity Radius/Ulna (deg.)	Preoperative Rotational Deformity Radius/Ulna (deg.)	Preoperative Distal Radioulnar Joint Instability	Preoperative Rotation (Pronation/ Supination) (deg.)	Postoperative Rotation (Pronation/ Supination) (deg.)	Complications
1	Distal radius malunion	18	28	Radius × 2	16/NA	27/NA	No	60/60	75/60	Transient radial sensory numbness
2	Madelung deformity	14	NA	Radius/ulna	15/22	11/5	Yes	10/80	20/85	None
3	Proximal radius malunion	14	60	Radius*	NA/NA	NA/NA	No	10/45	60/60	None
4	Distal radius/ulna malunion	13	9	Radius/ulna	14/17	4/31	Yes	90/90	90/90	Hypertrophic scar
5	Radial shaft malunion	12	9	Radius × 2	35/NA	50/NA	Yes	90/70	90/90	None
6	Distal radius/ulna malunion	7	12	Radius × 2/ ulna	27/16	34/3	Yes	30/80	90/90	None
7	MHE	15	NA	Radius/ulna	37/35	102/5	No	−40/80	25/60	Extensor pollicis longus muscle weakness
8	Traumatic loss of distal ulna	11	104	Radius/ulna	27/27	13/16	No	ND	35/70	None
9	Distal radius malunion	14	36	Radius × 2/ ulna	20/15	31/20	Yes	80/80	80/80	None
10	Distal radius/ulna malunion	11	29	Radius/ulna	8/12	3/15	Yes	80/80	80/80	None
11	Radius/ulna shaft malunion	9	6	Radius × 2/ ulna	14/32	37/14	No	40/20	70/70	Transient radial sensory numbness
12	MHE	17	NA	Radius/ ulna × 2	22/45	1/45	No	−90/90	0/90	None
13	Traumatic ulnar arrest	15	96	Radius/ulna	33/8	14/2	No	75/75	90/90	None
14	MHE	13	NA	Ulna†	22/45	NA/63	No	30/80	Not tested	None
15	Proximal radius/ulna malunion	10	12	Radius/ulna	31/16	11/2	No	15/0	55/80	None
16	Proximal ulna malunion	12	72	Ulna	NA/26	14/4	No	45/45	Not tested	None
17	Radius malunion (distal + shaft)	14	23	Radius × 2	25/NA	4/NA	Yes	80/80	80/80	Delayed union
18	Proximal radius malunion	14	48	Radius	0/NA	59/NA	No	35/12	45/60	None
19	Chronic Monteggia	14	72	Radius/ulna	NA/12	7/12	Yes	80/40	80/60	Delayed union

*The patient who also had a radial head replacement.
†The patient who also had distraction lengthening of the ulna.
MHE indicates multiple hereditary exostoses.

TABLE 3. Postoperative Results

Variables (deg.)	Sample Size (N)	Preoperative	Postoperative	*P
Total forearm range of motion	17	101	132.7	0.017
Radius angular deformity	15	23.1	8.6	0.003
Ulna angular deformity	14	23.4	7.6	0.002

*Significance determined using Wilcoxon signed-rank test with significance set at $P = 0.05$.

not provide a way to guide the osteotomy.[13] In 2003, Athwal et al[14] demonstrated a series of complex distal radius corrections in which the surgeries were planned using CT image data, with the plan then translated into the operating room using an intraoperative guidance system. The technique presented here represents the natural evolution of computer-assisted surgical planning, with a much simpler translation of the preoperative plan to the operating room. The guides are designed to fit in 1 specific location on 1 specific bone, making it simple for the surgeon to carry out the exact preoperative plan in the operating room. The computer modeling and 3-dimensional printing for these cases was accomplished in partnership with clinical engineers at Materialise NV, but commercially available software also exists to accomplish the same goal.[12]

In this series, those patients with forearm malunions who were lacking pronosupination gained on average 57 degrees of forearm rotation, for an average postoperative arc of rotation of 138 degrees. This corresponds to the improvement in forearm rotation reported using other osteotomy techniques. Miyake et al[15] have reported on a similar series of forearm malunions treated after skeletal maturity using 3-dimensional preoperative osteotomy planning, but without preoperative planning of plate and screw placement. For the 18 subjects in that series who had limited forearm rotation preoperatively, average forearm rotation improved from 76 to 152 degrees. Price and Knapp[8] reported on the surgical treatment of 9 forearm malunions using closing-wedge osteotomies at the site of maximal deformity, and rotational correction based on 2-dimensional radiographic landmarks. They noted an average gain of 102 degrees in the arc of forearm rotation postoperatively, to an average final arc of 165 degrees. In 2007, Van Geenan and Beselaar[9] reported on their technique of using K-wires to determine the amount of malrotation to be corrected, along with closing-wedge osteotomies. In their series of 21 malunions, the mean

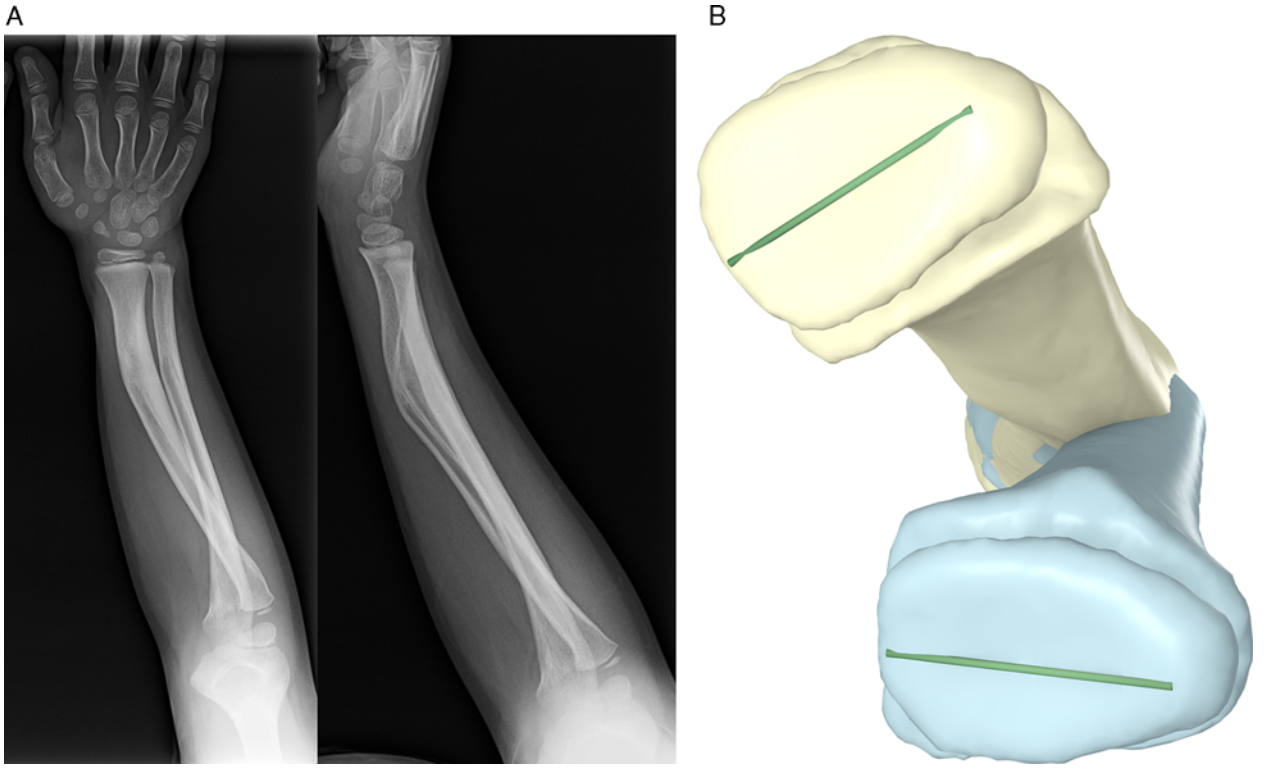

FIGURE 2. Plain radiographs and 3-dimensional model of a posttraumatic forearm deformity. A, The rotational deformity is not clearly evident on plain radiographs. B, A 3-dimensional model of the injured side versus a mirror image of the contralateral side clearly demonstrates a significant rotational deformity.

gain in forearm rotation was 85 degrees, to an average final arc of 140 degrees. In addition, we were able to resolve all cases of posttraumatic DRUJ instability via precise correction of the bony deformity, without any additional treatment of the soft tissues. This outcome parallels a recent cadaveric study, which demonstrated worsening DRUJ instability with increasing angulation of the distal radius, even in the presence of an intact triangular fibrocartilage complex.[16]

For posttraumatic deformities, it is generally accepted that >20 degrees of residual angulation in the radius or ulna is likely to lead to significant loss of forearm rotation.[1,17,18] This relationship, as well as the functional consequences of lost rotation, is less clear for nontraumatic etiologies. For example, children with MHE who have slowed growth of the ulna due to a distal ulna osteochondroma are known to be at risk for bowing of the radius and loss of forearm rotation.[19] However, this loss of rotation may not lead to significant disability.[20,21] In our series, improvement in forearm ROM seemed to be greater for posttraumatic deformities than for those due to MHE, although only 3 patients in the series had MHE. Further investigation of 3-dimensional osteotomies in children with MHE is needed to determine whether forearm function can be improved using this technique.

We present here the use of 3-dimensional computer modeling to achieve correction of pediatric forearm deformities of various etiologies. Of these, posttraumatic DRUJ instability seems an ideal indication. All 8 of our patients with this complaint had the instability resolve completely without the need for any soft-tissue procedures.

This study has several limitations. With the small number of patients treated so far, we cannot yet determine whether there will be a difference in outcomes based on etiology. Similarly, patients in this series ranged in age from 7 to 18 years. We do not yet know what the potential for recurrence is in children who were treated before physeal closure, especially in those with nontraumatic etiologies. In addition, this study concerns only the safety and short-term efficacy of this technique. Further study is required to evaluate the cost and value of this new technology along with long-term outcomes. ALthough we did not specifically evaluate the radiation dose of each CT scan in this study, the reported effective radiation dose of an adult elbow CT scan is 0.14 milliSevers (mSv), equivalent to 2 standard chest x-rays, whereas the reported effective radiation dose of an adult wrist and hand CT scan is 0.0.3 mSv, or less than half of a standard chest x-ray.[22]

Pediatric orthopaedics is defined by deformity correction, and the precision of correction required to restore proper forearm mechanics can be humbling. This study demonstrates a novel technique of preoperative computer modeling and patient-specific guides to correct complex forearm deformities. With 3-D printed guides the surgeon can accurately and efficiently translate a complex preoperative plan to a completed surgical correction, one that improves ROM and corrects DRUJ instability in children with these deformities.

ACKNOWLEDGMENTS

The authors would like to thank Alyssa Ricker, an employee of Materialise NV, for her assistance with editing and providing figures for this article.

REFERENCES

1. Matthews LS, Kaufer H, Garver DF, et al. The effect on supination-pronation of angular malalignment of fractures of both bones of the forearm: an experimental study. *J Bone Joint Surg Am*. 1982;64:14–17.
2. Dumont CE, Thalmann R, Macy JC. The effect of rotational malunion of the radius and ulna on supination and pronation. *J Bone Joint Surg Br*. 2002;84:1070–1074.
3. Evans EM. Rotational deformity in the treatment of fractures of both bones of the forearm. *J Bone Joint Surg*. 1945;27A:373–379.
4. Creasman C, Zaleske DJ, Ehrlich MG. Analyzing forearm fractures in children: the more subtle signs of impending problems. *Clin Orthop*. 1984;118:40–53.
5. Miyake J, Oka K, Kataoka T, et al. 3-Dimensional deformity analysis of malunited forearm diaphyseal fractures. *J Hand Surg Am*. 2013;38:1356–1365.
6. Price CT, Scott DS, Kurzner ME, et al. Malunited forearm fractures in children. *J Pediatr Orthop*. 1990;10:705–712.
7. Daruwalla JS. A study of radioulnar movements following fractures of the forearm in children. *Clin Orthop*. 1979;139:114–120.
8. Price CT, Knapp DR. Osteotomy for malunited forearm shaft fractures in children. *J Pediatr Orthop*. 2006;26:193–196.
9. Van Geenen RC, Besselaar PP. Outcome after corrective osteotomy for malunited fractures of the forearm sustained in childhood. *J Bone Joint Surg Br*. 2007;89:236–239.
10. Schweizer A, Fürnstahl P, Nagy L. Three-dimensional correction of distal radius intra-articular malunions using patient-specific drill guides. *J Hand Surg Am*. 2013;38:2339–2347.
11. Leong NL, Buijze GA, Fu EC, et al. Computer-assisted versus non-computer-assisted preoperative planning of corrective osteotomy for extra-articular distal radius malunions: a randomized controlled trial. *BMC Musculoskelet Disord*. 2010;11:282.
12. Kataoka T, Oka K, Miyake J, et al. 3-Dimensional prebent plate fixation in corrective osteotomy of malunited upper extremity fractures using a real-sized plastic bone model prepared by preoperative computer simulation. *J Hand Surg Am*. 2013;38:909–919.
13. Jupiter JB, Ruder J, Roth DA. Computer-generated bone models in the planning of osteotomy of multidirectional distal radius malunions. *J Hand Surg Am*. 1992;17:406–415.
14. Athwal GS, Ellis RE, Small CF, et al. Computer-assisted distal radius osteotomy. *J Hand Surg Am*. 2003;28:951–958.
15. Miyake J, Murase T, Oka K, et al. Computer-assisted corrective osteotomy for malunited diaphyseal forearm fractures. *J Bone Joint Surg Am*. 2012;94:e150.
16. Nishiwaki M, Welsh M, Gammon B, et al. Distal radioulnar joint kinematics in simulated dorsally angulated distal radius fractures. *J Hand Surg Am*. 2014;39:656–663.
17. Fuller DJ, McCollough CJ. Malunited fractures of the forearm in children. *J Bone Joint Surg Br*. 1982;64B:364–367.
18. Sarmiento A, Ebramzadeh E, Brys D, et al. Angular deformities and forearm function. *J Orthop Res*. 1992;10:121–133.
19. Gottschalk HP, Kanauchi Y, Bednar MS, et al. Effect of osteochondroma location on forearm deformity in patients with multiple hereditary osteochondromatosis. *J Hand Surg Am*. 2012;37:2286–2293.
20. Litzelmann E, Mazda K, Jehanno P, et al. Forearm deformities in hereditary multiple exostosis: clinical and functional results at maturity. *J Pediatr Orthop*. 2012;32:835–841.
21. Noonan KJ, Levenda A, Snead J, et al. Evaluation of the forearm in untreated adult subjects with multiple hereditary osteochondromatosis. *J Bone Joint Surg Am*. 2002;84:397–403.
22. Biswas D, Bible JE, Bohan M, et al. Radiation exposure from musculoskeletal computerized tomographic scans. *J Bone Joint Surg Am*. 2009;91:1882–1889.